Hindawi
Complexity
Volume 2018, Article ID 1814653, 9 pages
https://doi.org/10.1155/2018/1814653

WILEY | Hindawi

Research Article

Adaptive 3D Distance-Based Formation Control of Multiagent Systems with Unknown Leader Velocity and Coplanar Initial Positions

Xuejing Lan,[1,2] **Wenbiao Xu**,[3] **and Yun-Shan Wei**[1]

[1]*School of Mechanical and Electrical Engineering, Guangzhou University, Guangzhou 510006, China*
[2]*Center for Intelligent Equipment and Internet-Connected Systems, Guangzhou, China*
[3]*Guangdong Institute of Metrology, Guangzhou 510405, China*

Correspondence should be addressed to Yun-Shan Wei; weiys@gzhu.edu.cn

Received 11 May 2018; Accepted 25 July 2018; Published 6 September 2018

Academic Editor: Andy Annamalai

This paper considers the distributed 3-dimensional (3D) distance-based formation control of multiagent systems, where the agents are connected based on an acyclic minimally structural persistent (AMSP) graph. A parameter is designed according to the desired formation shape and is used to solve the problem that there are two formation shapes satisfying the same distance requirements. The unknown moving velocity of the leader agent is estimated adaptively by the followers requiring only the relative position measurements with respect to their local coordinate systems. In addition, the proposed formation controller provides a new way for the agent to leave the initial coplanar location. The 3D formation control law is globally asymptotically stable and has been demonstrated based on the Lyapunov theorem. Finally, two numerical simulations are presented to support the theoretical analysis.

1. Introduction

Cooperative control of a multiagent system has many applications such as surveillance, exploration, and search and rescue missions. In particular, formation control problem is one of the important aspects and has received significant attention recently with the development of the information communication technique [1–4].

According to the different requirements on the sensing capability and the interaction topology, the existing formation control schemes are categorized into position-based, displacement-based, and distance-based formation control. In the position-based formation control, the desired positions are given with respect to a global coordinate system, and the global position sensing is required [5]. The desired displacements are given and controlled in the displacement-based formation, where the relative positions of the neighboring agents are sensed with respect to a global coordinate system [6]. The distance-based formation is prescribed by the desired interagent distances, where the interagent distances are controlled and the relative positions of the neighboring agents are sensed with respect to their local coordinate systems [7–10]. The orientations of the local coordinate systems need not be aligned with each other. This means that a global sensing is not required in the distance-based formation control. Moreover, with the application of the rigid and persistent graph theory, only a part of the interagent distances needs to be controlled. Thus, the distance-based formation control has better cost-effectiveness than the other two approaches.

One of the hotspot problems in the distance-based formation control is how to maintain the formation shape, while the agents are tracking a reference trajectory or moving with a reference velocity [11]. A number of research works have considered the movement of formation in the displacement-based control. However, only few results in the distance-based control are available because of its extreme complexity in analysis [12, 13]. Further, in some real-world applications, such as the formation of unmanned flight vehicles and submarines [14, 15], the agents are actually moving in a 3-dimensional (3D) space, which will make the formation control scheme more complicated. Therefore, the study of 3D distance-based formation control is gaining

increasing attention [16, 17]. But they have not yet considered the movement of the formation. Then, Zhang et al. presented a 3D formation that can move with a given velocity while achieving the desired formation shape by directly adding a term of formation maneuvering velocity in the formation control law [18]. It is shown from the paper that the agents should know the reference velocity so as to remove the formation control error. In view of this, Kang et al. designed a distance-based formation control law in the leader-follower type with a moving leader [19, 20]. The follower agents in [19, 20] can estimate the velocity of the moving leader adaptively by only measuring the relative positions from their neighboring agents, which promotes the development of distance-based formation control. It is true that all the agents should not be collocated at a common point initially when using the steepest descent control law in the distance-based formation. The initial positions of the agents are usually set to noncollinear and close to the target formation shape [21, 22]. To solve this initial collinear problem, Park and Ahn modified the gradient control law by introducing a rotation matrix into the controller, which can change the descent direction and help the agents escape from the collinear position [23]. In [24], a formation control law was proposed based on two mutually perpendicular vectors, which provided a way for the agents to leave the initially collinear location. Another way to solve this problem is to set the initial velocity of the agent with a different orientation from the line [25]. Although the formation control problem with collinear initial positions of the agents has been solved [23–25], it is still challenging when the initial position of the agents is coplanar in the 3D distance-based formation.

In this paper, we aim to propose an adaptive 3D distance-based formation control law for a multiagent system with four kinds of agents, where the underlying graph of the formation is an acyclic minimally structural persistent (AMSP) graph. Compared with the global leader, first follower, and second follower, it is more difficult to design the controller for the ordinary follower, which follows three agents and has the problem of trapping in a plane. The proposed formation controller of the ordinary follower constructs a vector perpendicular to the plane determined by its three leaders, which provides a new way for the ordinary follower to leave the coplanar location. Moreover, a parameter is designed according to the desired formation shape and is used in the formation controller to solve the problem that there are two formation shapes satisfying the same distance requirements. The unknown moving velocity of the leader is adaptively estimated by the followers requiring only the relative position measurements with respect to their local coordinate systems. The 3D formation control law is globally asymptotically stable and has been demonstrated based on the Lyapunov theorem. The outline of this paper is listed as follows. Background and preliminaries are introduced in Section 2. The procedure of distributed formation control scheme design with the velocity estimator is presented in Section 3. Numerical simulations are completed in Section 4, and we reach a conclusion in Section 5.

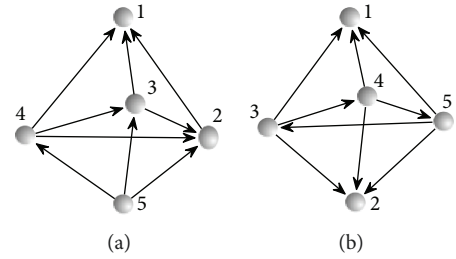

Figure 1: Examples of graph in a 3D space: (a) an acyclic minimally structural persistent graph; (b) minimally persistent but not structurally persistent graph.

2. Background and Preliminaries

2.1. Graph and Formation Structure. The formation problem of a multiagent system is modeled by a directed graph $\mathcal{G}$, which consists of a vertex set $\mathcal{V} = \{1, 2, \cdots, n\}$ and a directed edge set $\mathcal{E} = \{(i, j)\colon i, j \in \mathcal{V}, i \neq j\}$. The vertices represent the agents, and the weighted edges represent the interagent distance constraints. The neighboring set of agent i is defined as $\mathcal{N}_i = \{j \in \mathcal{V} \mid (i, j) \in \mathcal{E}\}$. A directed edge from i to j means that agent i can measure the relative position between agent i and j. Then, we call agent i a "follower" of agent j and correspondingly call agent j a "leader" of agent i. The formation shape can be maintained during any continuous motion, if the underlying graph is rigid and the distance constraints of each agent are satisfied. A formation graph is minimally persistent if it is rigid and constraint consistent with the minimum possible number of edges [26–28].

For a 3D minimally persistent formation, the sum of the degrees of freedoms (DOFs) of agents is always six [29]. Then, there exist various structures of the formation graph, according to the different distributions of these 6 DOFs among non-0-DOF agents. Moreover, the concept of structural persistence should be taken into consideration for 3D application [29]. For example, the graph in Figure 1(a) is an acyclic minimally structural persistent (AMSP) graph, while the graph in Figure 1(b) is minimally persistent but not structurally persistent with two free leaders.

In this paper, the AMSP graph is applied to construct the 3D leader-follower formation structure, which is the most convenient structure to design distributed control schemes. In the AMSP graph, there are one 3-DOF agent called the global leader, one 2-DOF agent called the first follower, one 1-DOF agent called the second follower, and some 0-DOF agents called ordinary followers.

2.2. Problem Statement. In the distance-based formation, the desired formation is prescribed by the desired interagent distances. The desired distance between agent i and agent j is denoted by $d_{ij} > 0$ and apparently $d_{ij} = d_{ji}$. It is assumed that each agent i measures the relative positions of its neighboring agents via an onboard sensor with respect to its local coordinate system ${}^{i}\sum$. The orientations of the local coordinate systems are not aligned with each other. All the agents move in a 3-dimensional space. Although the control law of each agent is implemented in ${}^{i}\sum$ in practice, it is more convenient to

represent the agents with respect to a global coordinate system ${}^{g}\sum$ for stability analysis. In addition, the state in ${}^{i}\sum$ can be transformed into ${}^{g}\sum$ by a suitable coordinate transformation. In this paper, the state of each agent will be represented with respect to ${}^{g}\sum$. The position and the velocity of agent i at time t in ${}^{g}\sum$ are denoted by $p_i(t) = [X_i, Y_i, Z_i]^{\mathrm{T}} \in R^3$ and $v_i(t) = [V_i^X, V_i^Y, V_i^Z]^{\mathrm{T}} \in R^3$, respectively. The dynamics of agent i is modeled as a single integrator:

$$\dot{p}_i(t) = u_i(t), \tag{1}$$

where $u_i \in R^3$, $i = 2, \ldots, n$, is the control input of agent i. $\overrightarrow{z}_{ij} \in R^3$ is used to represent the relative position vector as follows:

$$\overrightarrow{z}_{ij} = p_i - p_j. \tag{2}$$

In this paper, only the relative position $\overrightarrow{z}_{ij}$ can be measured directly by agent j, where agent j is a follower of agent i. A follower is responsible for maintaining the desired distances from its leaders, while the leader does not perform any action to maintain the distance. Then, the formation control procedure is to design a decentralized formation control law for each follower agent such that

$$\lim_{t\to\infty} \left\| \overrightarrow{z}_{ij} \right\| = d_{ij}. \tag{3}$$

3. Results

In this section, firstly, we design the formation control laws for an AMSP formation with four agents (one global leader agent v_1, one first follower agent v_2, one second follower agent v_3, and one ordinary follower agent v_4). Then, the proposed formation control laws are extended to an AMSP formation with $n(n \geq 4)$ agents.

3.1. Controller Design for Formation with Four Agents. The global leader does not follow any other agents and determines where the entire formation goes. The control input for the global leader is shown as

$$u_1 = v, \tag{4}$$

where v is the designed velocity of the entire formation. We consider the situation that the velocity of the leader is not known to all the followers. And an adaptive method is applied to estimate the velocity of the leader.

The first follower only follows the global leader and maintains the desired distance towards the global leader. The control law with an estimator for the first follower is shown as follows:

$$u^2 = \hat{v}_2 + e_{12}\overrightarrow{z}_{12}, \dot{\hat{v}}_2 = \overrightarrow{z}_{12}e_{12}, \tag{5}$$

where $e_{12} = \left\| \overrightarrow{z}_{12} \right\|^2 - d_{12}^2$ and $\hat{v}_2$ is the estimation for v by the first follower.

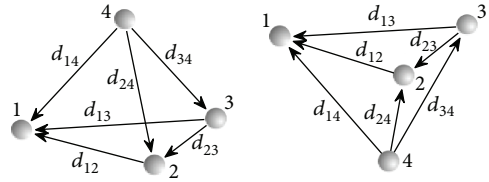

Figure 2: Two different formations for the ordinary follower that satisfy the same distance requirements: (a) orientation 1; (b) orientation 2.

The second follower follows the global leader and the first follower. The control law with an estimator for the second follower is shown as follows:

$$u_3 = \hat{v}_3 + \overrightarrow{z}_{13}e_{13} + \overrightarrow{z}_{23}e_{13}, \dot{\hat{v}} = \overrightarrow{z}_{13}e_{13} + \overrightarrow{z}_{23}e_{23}, \tag{6}$$

where $e_{13} = \left\| \overrightarrow{z}_{13} \right\|^2 - d_{13}^2$, $e_{23} = \left\| \overrightarrow{z}_{23} \right\|^2 - d_{23}^2$, and $\hat{v}_3$ is the estimation for v by the second follower. In addition, the convergences of the first follower and second follower to the desired formation have been proven in [20].

Assumption 1. In this paper, the desired formation is realizable. All the corresponding desired distances satisfy the triangular inequality constraints. For example, $d_{12} < d_{13} + d_{23}, d_{23} < d_{12} + d_{13}$ and $d_{13} < d_{12} + d_{23}$. Further, the first follower and the second follower have converged to the desired formation by the controllers and estimators. That is, $\| \overrightarrow{z}_{12} \| \to d_{12}$, $\| \overrightarrow{z}_{13} \| \to d_{13}$, $\| \overrightarrow{z}_{23} \| \to d_{23}$, $\dot{p}_2 \to v$, and $\dot{p}_3 \to v$ are known.

Therefore, in this paper, we focus on designing the controller for the ordinary follower, which follows three agents and measures the relative positions of the three neighbors. It should be noted that the formation is not globally rigid, as the agents are connected based on an AMSP graph. Obviously, there exist two different formations for the ordinary follower that satisfy the same distance requirements in a 3D space, shown in Figure 2. In the sequel, we call the formation in Figure 2(a) as orientation 1 and the formation in Figure 2(b) as orientation 2. To achieve the global convergence of the system, a new formation control law with an adaptive estimator for the ordinary follower is proposed as follows:

$$u_4 = e_{14} \cdot \left(\overrightarrow{z}_{12} \times \overrightarrow{z}_{13} \right) + e_{24} \cdot \overrightarrow{z}_{12} + e_{34} \cdot \overrightarrow{z}_{13} + \hat{v}_4, \tag{7}$$

$$\dot{\hat{v}}_4 = e_{14} \cdot \left(\overrightarrow{z}_{12} \times \overrightarrow{z}_{13} \right) + e_{24} \cdot \overrightarrow{z}_{12} + e_{34} \cdot \overrightarrow{z}_{13}, \tag{8}$$

$$e_{14} = \left(\overrightarrow{z}_{12} \times \overrightarrow{z}_{13} \right) \cdot \overrightarrow{z}_{14} - E_{14}, \tag{9}$$

$$e_{24} = \overrightarrow{z}_{24} \cdot \overrightarrow{z}_{12} - E_{24}, \tag{10}$$

$$e_{34} = \overrightarrow{z}_{34} \cdot \overrightarrow{z}_{13} - E_{34}, \tag{11}$$

where $\widehat{v}_4$ is the estimation for v by the ordinary follower. The cross product $(\overrightarrow{z}_{12} \times \overrightarrow{z}_{13})$ is a vector perpendicular to the plane determined by $\overrightarrow{z}_{12}$ and $\overrightarrow{z}_{13}$, which provides a way for the ordinary follower to escape from the coplanar position. E_{14} is the inner product of $(\overrightarrow{z}_{12} \times \overrightarrow{z}_{13})$ and $\overrightarrow{z}_{14}$ when the expected formation is achieved, E_{24} is the inner product of $\overrightarrow{z}_{24}$ and $\overrightarrow{z}_{12}$ when the expected formation is achieved, and E_{34} is the inner product of $\overrightarrow{z}_{34}$ and $\overrightarrow{z}_{13}$ when the expected formation is achieved. E_{24} and E_{34} for the two different formations are the same as follows:

$$\begin{aligned} E_{24} &= \frac{d_{24}^2 - d_{12}^2 - d_{14}^2}{2}, \\ E_{34} &= \frac{d_{34}^2 - d_{13}^2 - d_{14}^2}{2}. \end{aligned} \tag{12}$$

E_{14} is designed according to the desired formation shape and is used in the formation controller to solve the problem that there are two different formation shapes satisfying the same distance requirements. When the expected formation is as shown in Figure 2(a), E_{14} is designed by (13). When the expected formation is as shown in Figure 2(b), E_{14} is designed by (14).

$$E_{14} = 6 \cdot V, \tag{13}$$

$$E_{14} = -6 \cdot V, \tag{14}$$

where V is the expected volume of the tetrahedron constructed by the agents v_1, v_2, v_3, and v_4, which can be calculated by the Carley-Menger determinant:

$$V = \frac{1}{288} \sqrt{\begin{vmatrix} 0 & 1 & 1 & 1 & 1 \\ 1 & 0 & d_{12}^2 & d_{13}^2 & d_{14}^2 \\ 1 & d_{12}^2 & 0 & d_{23}^2 & d_{24}^2 \\ 1 & d_{13}^2 & d_{23}^2 & 0 & d_{34}^2 \\ 1 & d_{14}^2 & d_{24}^2 & d_{34}^2 & 0 \end{vmatrix}}. \tag{15}$$

Lemma 3.1. *The distance error and velocity estimation error of the ordinary follower are bounded (i.e., e_{14}, e_{24}, e_{34}, and $\|v_1 - \widehat{v}_4\|$ are bounded).*

Proof 1. Define the following Lyapunov function:

$$V_p = e_{14}^2 + e_{24}^2 + e_{34}^2 + \|v - \widehat{v}_4\|^2, \tag{16}$$

which is continuously differentiable and satisfies that $V_p \geq 0$ with equality if and only if $e_{14} = 0$, $e_{24} = 0$, $e_{34} = 0$, and $\|v_1 - \widehat{v}_4\| = 0$. Based on Assumption 1, it is known that $\overrightarrow{z}_{12}$ and $\overrightarrow{z}_{13}$ are not collinear. Then, $\overrightarrow{z}_{12} \times \overrightarrow{z}_{13}$ is perpendicular to the planar defined by $\overrightarrow{z}_{12}$ and $\overrightarrow{z}_{13}$. Thus, the three noncoplanar vectors of $\overrightarrow{z}_{12} \times \overrightarrow{z}_{13}$, $\overrightarrow{z}_{12}$, and $\overrightarrow{z}_{13}$ can form a base of R^3 space. Then, v and $\widehat{v}_4$ can be reexpressed as follows:

$$v = \alpha \cdot (\overrightarrow{z}_{12} \times \overrightarrow{z}_{13}) + \beta \cdot \overrightarrow{z}_{12} + \chi \cdot \overrightarrow{z}_{13}, \tag{17}$$

$$\widehat{v}_4 = \widehat{\alpha} \cdot (\overrightarrow{z}_{12} \times \overrightarrow{z}_{13}) + \widehat{\beta} \cdot \overrightarrow{z}_{12} + \widehat{\chi} \cdot \overrightarrow{z}_{13}, \tag{18}$$

where α, β, and χ are the corresponding components of v, while $\widehat{\alpha}$, $\widehat{\beta}$, and $\widehat{\chi}$ are the corresponding components of $\widehat{v}_4$. Then,

$$\begin{aligned} V_p &= e_{14}^2 + e_{24}^2 + e_{34}^2 + \left\| (\alpha - \widehat{\alpha}) \cdot (\overrightarrow{z}_{12} \times \overrightarrow{z}_{13}) \right. \\ &\quad \left. + \left(\beta - \widehat{\beta}\right) \cdot \overrightarrow{z}_{12} + (\chi - \widehat{\chi}) \cdot \overrightarrow{z}_{13} \right\|^2 \\ &\leq e_{14}^2 + e_{24}^2 + e_{34}^2 + \left\| (\alpha - \widehat{\alpha}) \cdot (\overrightarrow{z}_{12} \times \overrightarrow{z}_{13}) \right\|^2 \\ &\quad + \left\| \left(\beta - \widehat{\beta}\right) \cdot \overrightarrow{z}_{12} \right\|^2 + \left\| (\chi - \widehat{\chi}) \cdot \overrightarrow{z}_{13} \right\|^2 \\ &= V_1 + V_2 + V_3 \triangleq V_\Theta, \end{aligned} \tag{19}$$

where

$$\begin{aligned} V_1 &= e_{14}^2 + \left\| (\alpha - \widehat{\alpha}) \cdot (\overrightarrow{z}_{12} \times \overrightarrow{z}_{13}) \right\|^2, \\ V_2 &= e_{24}^2 + \left\| \left(\beta - \widehat{\beta}\right) \cdot \overrightarrow{z}_{12} \right\|^2, \\ V_3 &= e_{34}^2 + \left\| (\chi - \widehat{\chi}) \cdot \overrightarrow{z}_{13} \right\|^2. \end{aligned} \tag{20}$$

The time derivative of V_1 is

$$\begin{aligned} \dot{V}_1 &= 2e_{14}\dot{e}_{14} - 2e_{14}(\alpha - \widehat{\alpha}) \cdot \left\| \overrightarrow{z}_{12} \times \overrightarrow{z}_{13} \right\|^2 \\ &= 2e_{14}\left(\alpha \cdot \left\| \overrightarrow{z}_{12} \times \overrightarrow{z}_{13} \right\|^2 - e_{14} \right. \\ &\quad \left. \cdot \left\| \overrightarrow{z}_{12} \times \overrightarrow{z}_{13} \right\|^2 - (\overrightarrow{z}_{12} \times \overrightarrow{z}_{13}) \cdot \widehat{v} \right) \\ &\quad - 2e_{14}(\alpha - \widehat{\alpha}) \cdot \left\| \overrightarrow{z}_{12} \times \overrightarrow{z}_{13} \right\|^2 \\ &= 2e_{14}\left(\alpha \cdot \left\| \overrightarrow{z}_{12} \times \overrightarrow{z}_{13} \right\|^2 - e_{14} \right. \\ &\quad \left. \cdot \left\| \overrightarrow{z}_{12} \times \overrightarrow{z}_{13} \right\|^2 - (\overrightarrow{z}_{12} \times \overrightarrow{z}_{13}) \right. \\ &\quad \left. \cdot \left[\widehat{\alpha} \cdot (\overrightarrow{z}_{12} \times \overrightarrow{z}_{13}) + \widehat{\beta} \cdot \overrightarrow{z}_{12} + \overline{\widehat{\chi}} \cdot \overrightarrow{z}_{13} \right] \right) \\ &\quad - 2e_{14}(\alpha - \widehat{\alpha}) \cdot \left\| \overrightarrow{z}_{12} \times \overrightarrow{z}_{13} \right\|^2 \\ &= 2e_{14}\left((\alpha - e_{14} - \widehat{\alpha}) \cdot \left\| \overrightarrow{z}_{12} \times \overrightarrow{z}_{13} \right\|^2 \right) \\ &\quad - 2e_{14}(\alpha - \widehat{\alpha}) \cdot \left\| \overrightarrow{z}_{12} \times \overrightarrow{z}_{13} \right\|^2 \\ &= -2e_{14}^2 \cdot \left\| \overrightarrow{z}_{12} \times \overrightarrow{z}_{13} \right\|^2 \leq 0. \end{aligned} \tag{21}$$

The time derivative of V_2 is

$$\begin{aligned} \dot{V}_2 &= 2e_{24}\dot{e}_{24} - 2e_{24}\left(\beta - \widehat{\beta}\right) \cdot \left\| \overrightarrow{z}_{12} \right\|^2 \\ &= 2e_{24}\left(\overrightarrow{z}_{12} \cdot \left(\beta \cdot \overrightarrow{z}_{12} - e_{24} \cdot \overrightarrow{z}_{12} - \widehat{\beta} \cdot \overrightarrow{z}_{12} \right) \right) \\ &\quad - 2e_{24}\left(\beta - \widehat{\beta}\right) \cdot \left\| \overrightarrow{z}_{12} \right\|^2 \\ &= 2e_{24}\left(\left(\beta - e_{24} - \widehat{\beta}\right) \cdot \left\| \overrightarrow{z}_{12} \right\|^2 \right) \\ &\quad - 2e_{24}\left(\beta - \widehat{\beta}\right) \cdot \left\| \overrightarrow{z}_{12} \right\|^2 \\ &= -2e_{24}^2 \cdot \left\| \overrightarrow{z}_{12} \right\|^2 \leq 0. \end{aligned} \tag{22}$$

The time derivative of V_3 is

$$\begin{aligned}\dot{V}_3 &= 2e_{34}\dot{e}_{34} - 2e_{34}(\chi - \widehat{\chi}) \cdot \left\| \overrightarrow{z}_{13} \right\|^2 \\ &= 2e_{34}\left(\overrightarrow{z}_{13} \cdot \left(\chi \cdot \overrightarrow{z}_{13} - e_{34} \cdot \overrightarrow{z}_{13} - \widehat{\chi} \cdot \overrightarrow{z}_{13} \right) \right) \\ &\quad - 2e_{34}(\chi - \widehat{\chi}) \cdot \left\| \overrightarrow{z}_{13} \right\|^2 \\ &= 2e_{34}\left((\chi - e_{34} - \widehat{\chi}) \cdot \left\| \overrightarrow{z}_{13} \right\|^2 \right) \\ &\quad - 2e_{34}(\chi - \widehat{\chi}) \cdot \left\| \overrightarrow{z}_{13} \right\|^2 \\ &= -2e_{34}^2 \cdot \left\| \overrightarrow{z}_{13} \right\|^2 \le 0.\end{aligned} \tag{23}$$

Then, the time derivative of V_Θ is

$$\dot{V}_\Theta = \dot{V}_1 + \dot{V}_2 + \dot{V}_3 \le 0, \tag{24}$$

which is negative semidefinite. From (19), V_Θ *is* continuously differentiable and satisfies that $V_\Theta \ge 0$. Therefore, $V_\Theta(t) \le V_\Theta(0)$ is bounded. From (19), it holds that $V_p(t) \le V_\Theta(t) \le V_\Theta(0)$. In addition, V_p is continuously differentiable and satisfies that $V_p \ge 0$ from (16). Therefore, V_p is bounded, and hence e_{14}, e_{24}, e_{34}, and $\|v - v^4\|$ are bounded.

Lemma 3.2. *The distance errors converge to zero (i.e., $e_{14} \to 0$, $e_{24} \to 0$, and $e_{34} \to 0$ as $t \to \infty$).*

Proof 2. From the fact that $V_\Theta(t)$ is continuously differentiable and bounded in Lemma 3.1, $\int_0^t V_\Theta dt$ must converge to a constant. Then, applying Barbalat's lemma gives the condition $\lim_{t\to\infty} \dot{V}_\Theta = 0$ (i.e., $\lim_{t\to\infty} \dot{V}_1 + \dot{V}_2 + \dot{V}_3 = 0$). Based on Assumption 1, $\overrightarrow{z}_{12} \times \overrightarrow{z}_{13}$, $\overrightarrow{z}_{12}$, and $\overrightarrow{z}_{13}$ are not zero. Thus, we have $\lim_{t\to\infty} e_{14} = \lim_{t\to\infty} e_{24} = \lim_{t\to\infty} e_{34} = 0$.

Lemma 3.3. *The velocity estimation error of the ordinary follower converges to zero (i.e., $\widehat{v}_4 \to v$ as $t \to \infty$).*

Proof 3. Define a function Q_1 as follows:

$$Q_1 = \left(\overrightarrow{z}_{12} \times \overrightarrow{z}_{13} \right) \cdot \overrightarrow{z}_{14}. \tag{25}$$

Then, we have the time derivative of Q_1 which is

$$\begin{aligned}\dot{Q}_1 &= \alpha \cdot \left\| \overrightarrow{z}_{12} \times \overrightarrow{z}_{13} \right\|^2 - e_{14} \\ &\quad \cdot \left\| \overrightarrow{z}_{12} \times \overrightarrow{z}_{13} \right\|^2 - \left(\overrightarrow{z}_{12} \times \overrightarrow{z}_{13} \right) \cdot \widehat{v} \\ &= \alpha \cdot \left\| \overrightarrow{z}_{12} \times \overrightarrow{z}_{13} \right\|^2 - e_{14} \cdot \left\| \overrightarrow{z}_{12} \times \overrightarrow{z}_{13} \right\|^2 \\ &\quad - \left(\overrightarrow{z}_{12} \times \overrightarrow{z}_{13} \right) \cdot \left[\widehat{\alpha} \cdot \left(\overrightarrow{z}_{12} \times \overrightarrow{z}_{13} \right) \right. \\ &\quad \left. + \widehat{\beta} \cdot \overrightarrow{z}_{12} + \widehat{\chi} \cdot \overrightarrow{z}_{13} \right] \\ &= (\alpha - \widehat{\alpha} - e_{14}) \cdot \left\| \overrightarrow{z}_{12} \times \overrightarrow{z}_{13} \right\|^2.\end{aligned} \tag{26}$$

From (9), $Q_1 = (\overrightarrow{z}_{12} \times \overrightarrow{z}_{13}) \cdot \overrightarrow{z}_{14} \to E_{14}$ is obtained because $e_{14} \to 0$ is already verified in Lemma 3.2. Then, Q_1 is continuously differentiable and bounded. Thus, from Barbalat's lemma, $\dot{Q}_1 \to 0$ is obtained (i.e., $(\alpha - \widehat{\alpha} - e_{14}) \cdot \|\overrightarrow{z}_{12} \times \overrightarrow{z}_{13}\|^2 \to 0$). Based on Assumption 1, $\overrightarrow{z}_{12} \times \overrightarrow{z}_{13}$ is not zero. Further, $e_{14} \to 0$ is already proved. To satisfy $\dot{Q}_1 \to 0$, $\alpha - \widehat{\alpha}$ should converge to zero (i.e., $\widehat{\alpha} \to \alpha$). Define a function Q_2 as follows:

$$Q_2 = \overrightarrow{z}_{24} \cdot \overrightarrow{z}_{12}. \tag{27}$$

Then, we have the time derivative of Q_2 which is

$$\begin{aligned}\dot{Q}_2 &= \overrightarrow{z}_{12} \cdot \left(\beta \cdot \overrightarrow{z}_{12} - e_{24} \cdot \overrightarrow{z}_{12} - \widehat{\beta} \cdot \overrightarrow{z}_{12} \right) \\ &= \left(\beta - \widehat{\beta} - e_{24} \right) \cdot \left\| \overrightarrow{z}_{12} \right\|^2.\end{aligned} \tag{28}$$

From (10), $Q_2 = \overrightarrow{z}_{24} \cdot \overrightarrow{z}_{12} \to E_{24}$ is obtained because $e_{24} \to 0$ is already verified in Lemma 3.2. Then, Q_2 is continuously differentiable and bounded. Thus, from Barbalat's lemma, $\dot{Q}_2 \to 0$ is obtained (i.e., $(\beta - \widehat{\beta} - e_{24}) \|\overrightarrow{z}_{12}\|^2 \to 0$). Based on Assumption 1, $\overrightarrow{z}_{12}$ is not zero. Further, $e_{24} \to 0$ is already proved. To satisfy $\dot{Q}_2 \to 0$, $\beta - \widehat{\beta}$ should converge to zero (i.e., $\widehat{\beta} \to \beta$). Define a function Q_3 as follows:

$$Q_3 = \overrightarrow{z}_{34} \cdot \overrightarrow{z}_{13}. \tag{29}$$

Then, we have the time derivative of Q_3 which is

$$\begin{aligned}\dot{Q}_3 &= \overrightarrow{z}_{13} \cdot \left(\chi \cdot \overrightarrow{z}_{13} - e_{34} \cdot z_{13} - \widehat{\chi} \cdot \overrightarrow{z}_{13} \right) \\ &= (\chi - \widehat{\chi} - e_{34}) \cdot \left\| \overrightarrow{z}_{13} \right\|^2.\end{aligned} \tag{30}$$

From (11), $Q_3 = \overrightarrow{z}_{34} \cdot \overrightarrow{z}_{13} \to E_{34}$ is obtained because $e_{24} \to 0$ is already verified in Lemma 3.2. Then, Q_2 is continuously differentiable and bounded. Thus, from Barbalat's lemma, $\dot{Q}_3 \to 0$ is obtained (i.e., $(\chi - \widehat{\chi} - e_{34}) \cdot \|\overrightarrow{z}_{13}\|^2 \to 0$). Based on Assumption 1, $\overrightarrow{z}_{13}$ is not zero. Further, $e_{34} \to 0$ is already proved. To satisfy $\dot{Q}_3 \to 0$, $\chi - \widehat{\chi}$ should converge to zero (i.e., $\widehat{\chi} \to \chi$).

In conclusion, from (17) and (18), it is straightforward to obtain that $\widehat{v}_4 \to v$, because $\widehat{\alpha} \to \alpha$, $\widehat{\beta} \to \beta$, and $\widehat{\chi} \to \chi$.

Theorem 3.4. *The ordinary follower converges to the desired states by using the controller in (7) and estimator in (8) (i.e., $e_{14} \to 0$, $e_{24} \to 0$, $e_{34} \to 0$, $\widehat{v}_4 \to v$, and $\dot{p}_4 \to v$ as $t \to \infty$). That is, the system converges to the desired formation.*

Proof 4. From Lemma 3.1, it was proven that the distance errors e_{14}, e_{24}, and e_{34} and the velocity estimation error $\|v1 - \widehat{v}_4\|$ are bounded. Further, the convergence of distance errors e_{14}, e_{24}, and e_{34} to zero is obtained. In addition to the convergence of velocity estimator $\widehat{v}_4$ to v, from (7), the velocity of the ordinary follower $\dot{p}_4$ converges to v. As a result, all

of the agents converge to the desired formation as follows: $\dot{p}_2 \to v$, $\dot{p}_3 \to v$, $\dot{p}_4 \to v$, $\|\overrightarrow{z}_{12}\| \to d_{12}$, $\|\overrightarrow{z}_{13}\| \to d_{13}$, $\|\overrightarrow{z}_{23}\| \to d_{23}$, $\|\overrightarrow{z}_{14}\| \to d_{14}$, $\|\overrightarrow{z}_{24}\| \to d_{24}$, and $\|\overrightarrow{z}_{34}\| \to d_{34}$.

3.2. Extension to n-Agent Case. Then, we extend the proposed formation control law to an AMSP formation with n ($n \geq 4$) agents. Based on the AMSP graph, each ordinary follower i ($4 \leq i \leq n$) has exactly three neighbors, which are denoted by j, k, and w ($1 \leq j, k, w \leq i-1$), respectively. Without loss of generality, d_{ji}, d_{ki}, and d_{wi} denote the expected distance between the corresponding agents, respectively. From the previous analysis, the convergence of four agents to the desired formation was achieved. Therefore, based on the control law designed for agent v_4 ((7) and (8)), the control law for agent v_i can be inferred inductively as follows:

$$\begin{aligned} u_i &= e_{ji} \cdot \left(\overrightarrow{z}_{jk} \times \overrightarrow{z}_{jw}\right) + e_{ki} \cdot \overrightarrow{z}_{jk} + e_{wi} \cdot \overrightarrow{z}_{jw} + \widehat{v}_i, \\ \dot{\widehat{v}}_i &= e_{ji} \cdot \left(\overrightarrow{z}_{jk} \times \overrightarrow{z}_{jw}\right) + e_{ki} \cdot \overrightarrow{z}_{jk} + e_{wi} \cdot \overrightarrow{z}_{jw}, \\ e_{ji} &= \left(\overrightarrow{z}_{jk} \times \overrightarrow{z}_{jw}\right) \cdot \overrightarrow{z}_{ji} - E_{ji}, \\ e_{ki} &= \left(\overrightarrow{z}_{ki} \cdot \overrightarrow{z}_{jk}\right) - E_{ki}, \\ e_{wi} &= \left(\overrightarrow{z}_{wi} \cdot \overrightarrow{z}_{jw}\right) - E_{wi}, \end{aligned} \tag{31}$$

where $\widehat{v}_i$ is the estimation for v by agent v_i. E_{ji} is the inner product of $(\overrightarrow{z}_{jk} \times \overrightarrow{z}_{jw})$ and $\overrightarrow{z}_{ji}$ when the expected formation is achieved, E_{ki} is the inner product of $\overrightarrow{z}_{ki}$ and $\overrightarrow{z}_{jk}$ when the expected formation is achieved, and E_{wi} is the inner product of $\overrightarrow{z}_{wi}$ and $\overrightarrow{z}_{jw}$ when the expected formation is achieved. E_{ki} and E_{wi} for the two different formations are the same and calculated as follows:

$$\begin{aligned} E_{ki} &= \frac{d_{ki}^2 - d_{jk}^2 - d_{ji}^2}{s}, \\ E_{wi} &= \frac{d_{wi}^2 - d_{jw}^2 - d_{ji}^2}{2}. \end{aligned} \tag{32}$$

E_{ji} is designed according to the desired formation shape and is used in the formation controller to solve the problem that there are two different formation shapes satisfying the same distance requirements. When the expected formation is as shown in Figure 2(a), E_{ji} is designed by (33). When the expected formation is as shown in Figure 2(b), E_{ji} is designed by (34).

$$E_{ji} = 6 \cdot V_i, \tag{33}$$

$$E_{ji} = -6 \cdot V_i, \tag{34}$$

where V_i is the expected volume of the tetrahedron constructed by the agents v_j, v_k, v_w, and v_i, which can be calculated by the Carley-Menger determinant:

$$V_i = \frac{1}{288} \sqrt{\begin{vmatrix} 0 & 1 & 1 & 1 & 1 \\ 1 & 0 & d_{jk}^2 & d_{jw}^2 & d_{ji}^2 \\ 1 & d_{jk}^2 & 0 & d_{kw}^2 & d_{ki}^2 \\ 1 & d_{jw}^2 & d_{kw}^2 & 0 & d_{wi}^2 \\ 1 & d_{ji}^2 & d_{ki}^2 & d_{wi}^2 & 0 \end{vmatrix}}. \tag{35}$$

Assume that the $n-1$ agents constructed by an AMSP graph converge to the desired formation. Add a new agent to the graph of $n-1$ agents.

Then, the graph of n agents is still an AMSP graph, as the added agent follows three agents. The neighbors of the added agent belong to the graph of $n-1$ agents and converge to the desired formation as assumed. Then, the lemmas and theorems in Section 3 can be applied to the added agent by replacing the name of the agent. As a result, the n agents converge to the desired formation if the $n-1$ agents converge. Since both the basis and the inductive steps have been performed, by mathematical induction, the agents globally converge to the desired formation under the control law with an adaptive estimator.

4. Simulations

In this section, two simulations are presented to support our theoretical analysis. Firstly, we will show that two different formation shapes that satisfy the same distance requirements are achieved, respectively. Then, the simulation verifies that the ordinary follower can leave the initial coplanar location even when the velocity of the leader agent is in the same initial plane.

4.1. Two Different Formation Shapes. The initial positions of the five agents are given in a plane: $p_i(0)[2\cos((2\pi/5)i), 2\sin((2\pi/5)i), 0]^{\mathrm{T}}$, $i = 1, 2, 3, 4, 5$. The velocity of the leader agent is given as $v = [-1.5, -1, 0.5]^{\mathrm{T}}$. The desired distances between agents are assigned as follows: $d_{12} = d_{13} = d_{23} = 2\sqrt{23}$, $d_{14} = d_{24} = d_{34} = 2\sqrt{25}$, and $d_{15} = d_{25} = d_{35} = 2\sqrt{2}$. Then, the parameters are calculated as follows: $E_{24} = E_{34} = -6$, $V_4 = 4\sqrt{3}$, $E_{25} = E_{35} = -6$, and $V_5 = 2\sqrt{3}$. It is clear that the underlying graph of the desired formation is an AMSP graph, and there exist two different formations that satisfy the same distance requirements, which can be achieved based on the proposed control law as follows.

Case 1. Agent v_4 and agent v_5 are set to the same Orientation 1. Then, $E_{14} = 6 \cdot V_4 = 24\sqrt{3}$ and $E_{15} = 6 \cdot V_5 = 12\sqrt{3}$. The trajectories of agents in a 3D space are illustrated in Figure 3. It shows that agent v_4 and agent v_5 are on the same side of the plane determined by the agents v_1, v_2, and v_3.

Case 2. Agent v_4 is set to Orientation 2, while agent v_5 is set to Orientation 1. Then, $E_{14} = -6 \cdot V_4 = -24\sqrt{3}$ and $E_{15} = 6 \cdot V_5 = 12\sqrt{3}$. The trajectories of agents in a 3D space are shown in Figure 4. It shows that agent v_4 and agent v_5 are

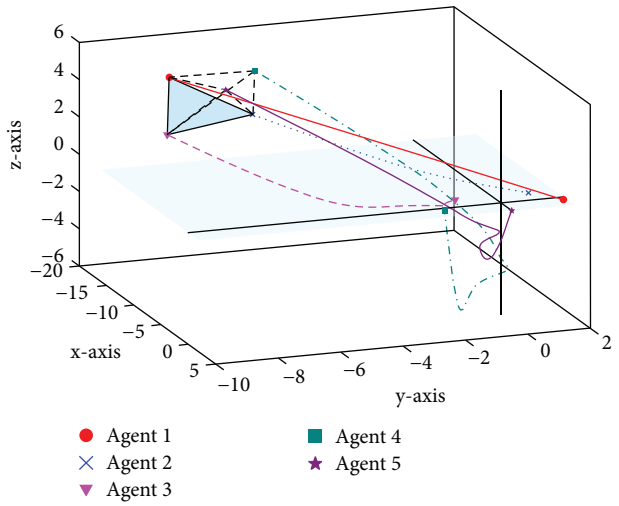

Figure 3: Trajectories of agents in a 3D space: agent v_4 and agent v_5 are in the same Orientation 1.

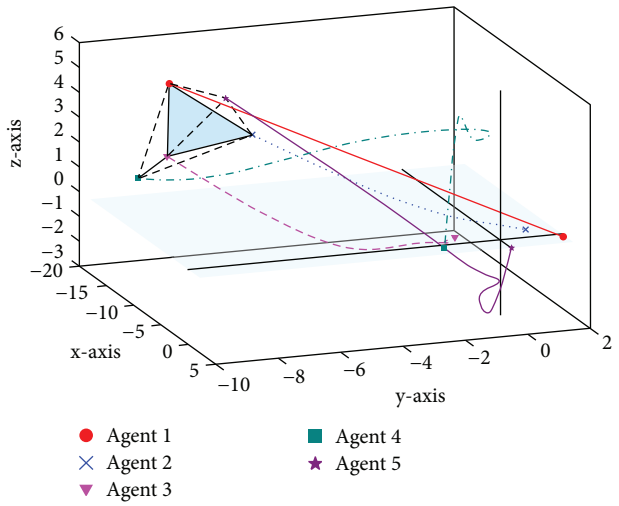

Figure 4: Trajectories of agents in a 3D space: agent v_4 is in Orientation 2, while agent v_5 is in Orientation 1.

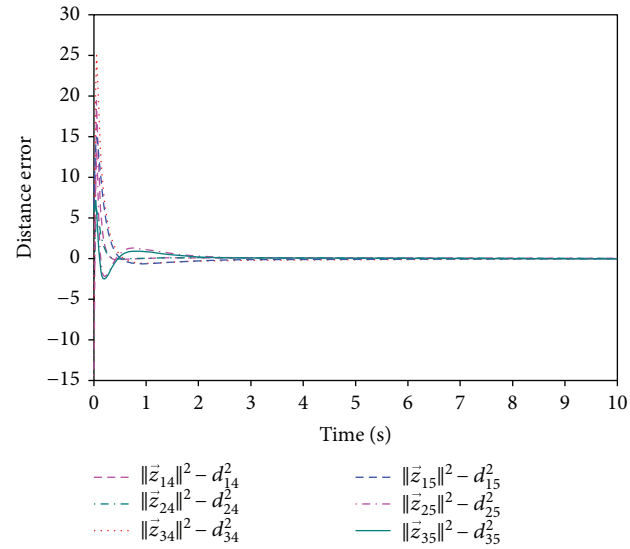

Figure 5: Distance errors: agent v_4 and agent v_5 are in the same Orientation 1.

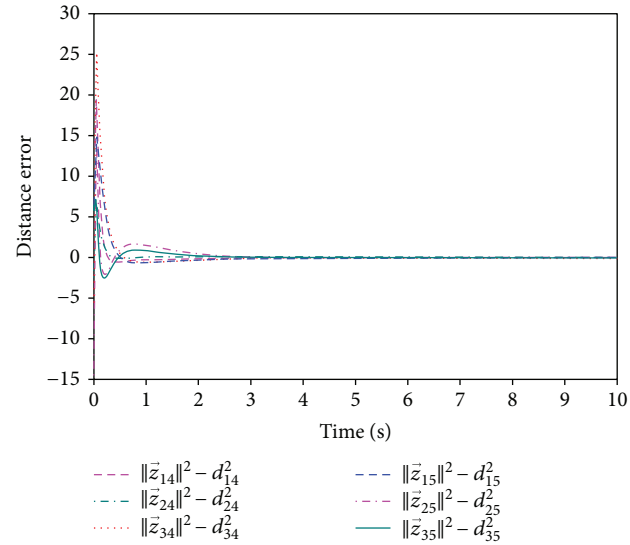

Figure 6: Distance errors: agent v_4 is in Orientation 2, while agent v_5 is in Orientation 1.

on the different sides of the plane determined by the agents v_1, v_2, and v_3.

It is shown from Case 1 and Case 2 that the two different formation shapes satisfying the same distance requirements can be achieved by designing different E_{14} and E_{15}. Further, the five agents approach the desired formation and maintain the formation shape while moving. The distance errors of the formation converge to zero quickly as shown with time in Figures 5 and 6.

4.2. Escape from the Initial Coplanar Position. As shown in Section 4.1, the agents can leave the initial coplanar location for the reason that the velocity of the leader agent is not in the plane. Moreover, based on the proposed formation controller, the ordinary follower can leave the initial coplanar location even when the velocity of the leader agent is also in the plane. Thus, in this section, the velocity of the leader agent is set as $v = [-1.5, -1, 0]^{\mathrm{T}}$. The other simulation conditions are set the same as those of Case 2 in Section 4.1. Then, the trajectories of agents in a 3D space are illustrated in Figure 7. It shows that agent v_4 and agent v_5 leave the initial coplanar location and approach the desired formation. The distance errors of the formation converge to zero quickly as shown with time in Figure 8.

5. Conclusion

In this paper, we investigate a decentralized 3D formation control law for a multiagent system. The proposed approach can achieve the different formation shapes that satisfy the same distance requirements, which extends the existing

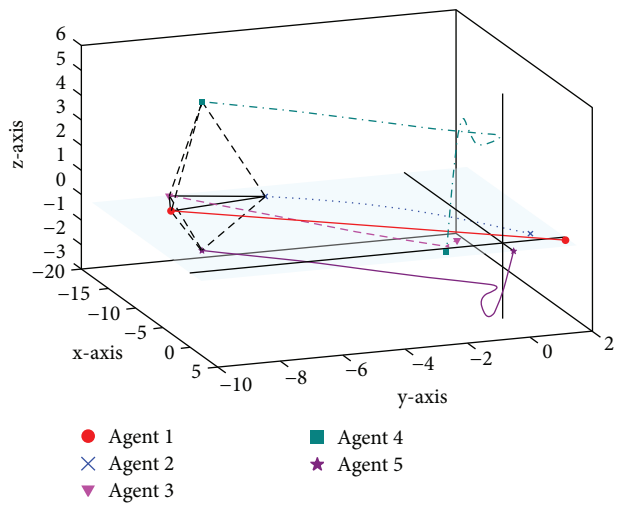

Figure 7: Trajectories of agents in a 3D space: the velocity of the leader agent is in the initial coplanar plane.

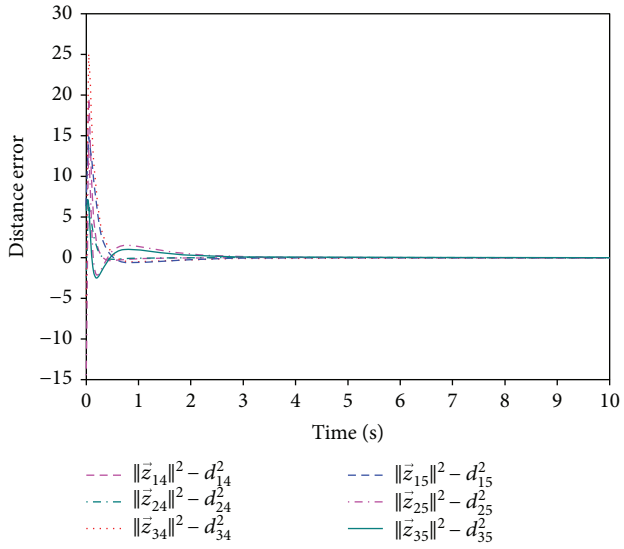

Figure 8: Distance errors: the velocity of the leader agent is in the initial coplanar plane.

distance-based 3D formation control laws. Although the underlying AMSP graph of the formation is not globally rigid, the multiagent system is still globally asymptotically stable. Moreover, a stable 3D formation motion can be realized, even when the initial positions of the agents are coplanar and the velocity of the leader agent is also in the plane. The performed numerical simulation results show the effectiveness of the formation control strategy.

In the future, we will further design more advanced formation control algorithms with robustness in mind. With the development of the adaptive neural network [30, 31], learning control [32], adaptive observer, and parameter estimation [33–35], the dynamics of the agent can be extended to the scenarios involving unknown nonlinear dynamics and external disturbances to further validate this formation control scheme.

Data Availability

The data used to support the findings of this study are available from the corresponding author upon request.

Conflicts of Interest

The authors declare that they have no conflicts of interest.

Acknowledgments

This work was supported by the National Natural Science Foundation of China (Grant no. 61473124) and Scientific Research Foundation of Guangzhou University (Grant no. 2700050356).

References

[1] Y.-Y. Chen and Y.-P. Tian, "Formation tracking and attitude synchronization control of underactuated ships along closed orbits," *International Journal of Robust and Nonlinear Control*, vol. 25, no. 16, pp. 3023–3044, 2015.

[2] Z. Lin, L. Wang, Z. Han, and M. Fu, "A graph Laplacian approach to coordinate-free formation stabilization for directed networks," *IEEE Transactions on Automatic Control*, vol. 61, no. 5, pp. 1269–1280, 2016.

[3] K. Sakurama, S. I. Azuma, and T. Sugie, "Multi-agent coordination to high-dimensional target subspaces," *IEEE Transactions on Control of Network Systems*, vol. 5, no. 1, pp. 345–358, 2018.

[4] S. L. Dai, S. He, H. Lin, and C. Wang, "Platoon formation control with prescribed performance guarantees for USVs," *IEEE Transactions on Industrial Electronics*, vol. 65, no. 5, pp. 4237–4246, 2018.

[5] S. Li, J. Zhang, X. Li, F. Wang, X. Luo, and X. Guan, "Formation control of heterogeneous discrete-time nonlinear multiagent systems with un-certainties," *IEEE Transactions on Industrial Electronics*, vol. 64, no. 6, pp. 4730–4740, 2017.

[6] Z. Lin, B. Francis, and M. Maggiore, "State agreement for continuous-time coupled nonlinear systems," *SIAM Journal on Control and Optimization*, vol. 46, no. 1, pp. 288–307, 2007.

[7] X. Dong, J. Xi, G. Lu, and Y. Zhong, "Formation control for high-order linear time-invariant multiagent systems with time delays," *IEEE Transactions on Control of Network Systems*, vol. 1, no. 3, pp. 232–240, 2014.

[8] M. C. Park, K. Jeong, and H. S. Ahn, "Formation stabilization and resizing based on the control of inter-agent distances," *International Journal of Robust and Nonlinear Control*, vol. 25, no. 14, pp. 2532–2546, 2015.

[9] M. Aranda, G. Lopez-Nicolas, C. Sagues, and M. M. Zavlanos, "Distributed formation stabilization using relative position measurements in local coordinates," *IEEE Transactions on Automatic Control*, vol. 61, no. 12, pp. 3925–3935, 2016.

[10] K. K. Oh and H. S. Ahn, "Leader-follower type distance-based formation control of a group of autonomous agents," *International Journal of Control, Automation and Systems*, vol. 15, no. 4, pp. 1738–1745, 2017.

[11] H. G. de Marina, B. Jayawardhana, and M. Cao, "Distributed rotational and translational maneuvering of rigid formations and their applications," *IEEE Transactions on Robotics*, vol. 32, no. 3, pp. 684–697, 2016.

[12] B. Jiang, M. Deghat, and B. D. O. Anderson, "Simultaneous velocity and position estimation via distance-only measurements with application to multi-agent system control," *IEEE Transactions on Automatic Control*, vol. 62, no. 2, pp. 869–875, 2017.

[13] X. Ge and Q. L. Han, "Distributed formation control of networked multi-agent systems using a dynamic event-triggered communication mechanism," *IEEE Transactions on Industrial Electronics*, vol. 64, no. 10, pp. 8118–8127, 2017.

[14] X. J. Lan, Y. J. Wang, and L. Liu, "Dynamic decoupling tracking control for the polytopic LPV model of hypersonic vehicle," *Science China Information Sciences*, vol. 58, no. 9, pp. 1–14, 2015.

[15] X. J. Lan, L. Liu, and Y. J. Wang, "Online trajectory planning and guidance for reusable launch vehicles in the terminal area," *Acta Astronautica*, vol. 118, pp. 237–245, 2016.

[16] K. K. Oh and H. S. Ahn, "Local asymptotic convergence of a cycle-free persistent formation of double-integrators in three-dimensional space," in *2012 IEEE International Symposium on Intelligent Control*, pp. 692–696, Dubrovnik, Croatia, October 2012.

[17] Z. Lin, Z. Chen, and M. Fu, "A linear control approach to distributed multi-agent formations in d-dimensional space," in *52nd IEEE Conference on Decision and Control*, pp. 6049–6054, Florence, Italy, December 2013.

[18] P. Zhang, M. de Queiroz, and X. Cai, "Three-dimensional dynamic formation control of multi-agent systems using rigid graphs," *Journal of Dynamic Systems, Measurement, and Control*, vol. 137, no. 11, pp. 111006-111007, 2015.

[19] S. M. Kang, M. C. Park, B. H. Lee, and H. S. Ahn, "Distance-based formation control with a single moving leader," in *2014 American Control Conference*, pp. 305–310, Portland, OR, USA, June 2014.

[20] S. M. Kang and H. S. Ahn, "Design and realization of distributed adaptive formation control law for multi-agent systems with moving leader," *IEEE Transactions on Industrial Electronics*, vol. 63, no. 2, pp. 1268–1279, 2016.

[21] K. K. Oh and H. S. Ahn, "Distance-based undirected formations of single-integrator and double-integrator modeled agents in *n*-dimensional space," *International Journal of Robust and Nonlinear Control*, vol. 24, no. 12, pp. 1809–1820, 2014.

[22] Z. Sun, S. Mou, M. Deghat, and B. D. O. Anderson, "Finite time distributed distance-constrained shape stabilization and flocking control for *d*-dimensional undirected rigid formations," *International Journal of Robust and Nonlinear Control*, vol. 26, no. 13, pp. 2824–2844, 2016.

[23] M. C. Park and H. S. Ahn, "Distance-based acyclic minimally persistent formations with non-steepest descent control," *International Journal of Control, Automation and Systems*, vol. 14, no. 1, pp. 163–173, 2016.

[24] F. He, W. Chen, Y. Wang, Y. Yao, and L. Wang, "Distributed formation control of mobile autonomous agents using relative position measurements," *IET Control Theory & Applications*, vol. 7, no. 11, pp. 1540–1552, 2013.

[25] M. Deghat, B. D. O. Anderson, and Z. Lin, "Combined flocking and distance-based shape control of multi-agent formations," *IEEE Transactions on Automatic Control*, vol. 61, no. 7, pp. 1824–1837, 2016.

[26] J. M. Hendrickx, B. D. O. Anderson, J.-C. Delvenne, and V. D. Blondel, "Directed graphs for the analysis of rigidity and persistence in autonomous agent systems," *International Journal of Robust and Nonlinear Control*, vol. 17, no. 10-11, pp. 960–981, 2007.

[27] L. Xiaoyuan, L. Shaobao, and G. Xinping, "Automatic generation of minimally persistent formations using rigidity matrix," in *2009 IEEE Intelligent Vehicles Symposium*, pp. 1198–1203, Xi'an, China, June 2009.

[28] B. D. O. Anderson, C. Yu, B. Fidan, and J. M. Hendrickx, "Rigid graph control architectures for autonomous formations," *IEEE Control Systems Magazine*, vol. 28, no. 6, pp. 48–63, 2008.

[29] C. Yu, J. M. Hendrickx, B. Fidan, B. D. O. Anderson, and V. D. Blondel, "Three and higher dimensional autonomous formations: rigidity, persistence and structural persistence," *Automatica*, vol. 43, no. 3, pp. 387–402, 2007.

[30] Z. Zhao, J. Shi, X. Lan, X. Wang, and J. Yang, "Adaptive neural network control of a flexible string system with non-symmetric dead-zone and output constraint," *Neurocomputing*, vol. 283, pp. 1–8, 2018.

[31] C. Yang, X. Wang, Z. Li, Y. Li, and C. Y. Su, "Teleoperation control based on combination of wave variable and neural networks," *IEEE Transactions on Systems Man and Cybernetics Systems*, vol. 47, no. 8, pp. 2125–2136, 2017.

[32] B. Xu and Y. Shou, "Composite learning control of MIMO systems with applications," *IEEE Transactions on Industrial Electronics*, vol. 65, no. 8, pp. 6414–6424, 2018.

[33] J. Huang, S. Ri, L. Liu, Y. Wang, J. Kim, and G. Pak, "Nonlinear disturbance observer-based dynamic surface control of mobile wheeled inverted pendulum," *IEEE Transactions on Control Systems Technology*, vol. 23, no. 6, pp. 2400–2407, 2015.

[34] C. Yang, Y. Jiang, W. He, J. Na, Z. Li, and B. Xu, "Adaptive parameter estimation and control design for robot manipulators with finite-time convergence," *IEEE Transactions on Industrial Electronics*, vol. 65, no. 10, pp. 8112–8123, 2018.

[35] J. Huang, Y. Wang, and T. Fukuda, "Set-membership-based fault detection and isolation for robotic assembly of electrical connectors," *IEEE Transactions on Automation Science and Engineering*, vol. 15, no. 1, pp. 160–171, 2018.